**Glycobiology** vol. 21 no. 8 pp. 1000–1009, 2011
doi:10.1093/glycob/cwr012
Advance Access publication on February 8, 2011

# Structure of a lectin with antitumoral properties in king bolete (*Boletus edulis*) mushrooms

**Michele Bovi[2], Maria E Carrizo[3], Stefano Capaldi[2], Massimiliano Perduca[2], Laurent R Chiarelli[4], Monica Galliano[4], and Hugo L Monaco[1,2]**

[2]Biocrystallography Laboratory, Department of Biotechnology, University of Verona, Ca Vignal 1, strada Le Grazie 15, 37134 Verona, Italy; [3]Departamento de Química Biológica, Facultad de Ciencias Químicas, Universidad Nacional de Córdoba C.P., 5016 Córdoba, Argentina; and [4]Department of Biochemistry "A. Castellani", University of Pavia, via Taramelli 3b, 27100 Pavia, Italy

*Received on December 21, 2010; revised on January 24, 2011; accepted on January 24, 2011*

**A novel lectin has been isolated from the fruiting bodies of the common edible mushroom *Boletus edulis* (king bolete, penny bun, porcino or cep) by affinity chromatography on a chitin column. We propose for the lectin the name BEL (*B. edulis* lectin). BEL inhibits selectively the proliferation of several malignant cell lines and binds the neoplastic cell-specific T-antigen disaccharide, Galβ1-3GalNAc. The lectin was structurally characterized: the molecule is a homotetramer and the 142-amino acid sequence of the chains was determined. The protein belongs to the saline-soluble family of mushroom fruiting body-specific lectins. BEL was also crystallized and its three-dimensional structure was determined by X-ray diffraction to 1.15 Å resolution. The structure is similar to that of *Agaricus bisporus* lectin. Using the appropriate co-crystals, the interactions of BEL with specific mono- and disaccharides were also studied by X-ray diffraction. The six structures of carbohydrate complexes reported here provide details of the interactions of the ligands with the lectin and shed light on the selectivity of the two distinct binding sites present in each protomer.**

*Keywords: Boletus edulis* / lectin / mushroom / structure / T-antigen

## Introduction

Lectins are proteins of non-immune origin devoid of any catalytic activity that reversibly bind mono- and oligosaccharides with high specificity and are involved, through sugar binding, in many fundamental biological processes such as, among others, cell-to-cell interactions and innate immunity (Sharon and Lis 2004; Sharon 2007). They are present in all kinds of organisms from viruses to man, were initially identified in the plant kingdom for their hemagglutinating activity and are now being widely used in basic and clinical research to develop new drugs for cancer therapy (Gonzàlez De Mejia and Prisecaru 2005), to treat microbial and viral infection (Sharon 2006; Wellens et al. 2008) and to fractionate hemopoietic stem cells for transplantation (Reisner et al. 1978).

Fungi are heterotrophic organisms with a chitinous cell wall that depend on symbiosis for their source of energy and have to specifically recognize their host for adhesion, a process which is often achieved through the recognition of glycoconjugates by a fungal lectin (Imberty et al. 2005). The first fungal lectin was discovered in the toxic fungus *Amanita phalloides* as a result of research in the field of toxic substances present in higher fungi (reviewed by Khan and Khan 2011). Ectomycorrhizal symbiosis is the way of association formed between fungi and the roots of plants in which the fungus obtains mono- and disaccharides from the roots providing in exchange the use of the mycelium's large surface area to absorb water and minerals from the soil, thus improving the mineral absorption capabilities of the plant root (Taylor and Alexander 2005). There are more than 140 mycorrhizal fungi with edible fruiting bodies (Hall et al. 1998), a group that includes some of the most expensive and globally diffused foods in the world (Hall et al. 2003). Among this group of mushrooms, the genus *Boletus* contains many members which are highly valued because they are edible and tasty, and several species that are closely related to each other and quite difficult to distinguish are often marketed together with the general name of *Boletus edulis* (Hall et al. 1998). The mushrooms from the genus *Boletus* have not yet been cultivated, whereas another common and widely diffused species, *Agaricus bisporus*, has, which explains why in most countries the volumes of *Agaricus* consumed are significantly higher (Hall et al. 2003). *Agaricus bisporus* contains a lectin (ABL) that has the remarkable property of binding selectively and with high affinity, the Thomsen–Friedenreich antigen or T-antigen. The T-antigen is a disaccharide, Galβ1-3GalNAc, linked to either serines or threonines on cell surface glycoproteins and hidden in healthy cells while exposed in a high percentage of human carcinomas and other neoplastic tissues (Springer 1984, 1997). ABL has the property of reversibly inhibiting the proliferation of malignant epithelial cell lines

[1]To whom correspondence should be addressed: Tel: +39-045-8027-903; Fax: +39-045-8027-929; e-mail: monaco@sci.univr.it

without any apparent cytotoxicity for normal cells (Yu et al. 1993). This effect is thought to be a consequence of the selective blocking by ABL of the nuclear localization sequence-dependent protein import, essential for cell functioning (Yu et al. 1999, 2000; Yu 2007). Following our determination of the three-dimensional structure of ABL by X-ray crystallography, the characterization of the T-antigen-binding site and the discovery that the lectin has two distinct binding sites for *N*-acetylgalactosamine and *N*-acetylglucosamine (Carrizo et al. 2005), we decided to explore the possibility of the existence of a lectin with similar properties in the genus *Boletus* as well. We reasoned that the second binding site probably bound polymers of *N*-acetylglucosamine and the most common of these polymers is chitin, a constituent of the fungal cell wall and therefore present in high quantities in fungal cells (Wu et al. 2004). Therefore, we devised a protocol that uses as its major purification step the specific affinity for a chitin resin and, in this way, we isolated the lectin that we propose to call *B. edulis* lectin (BEL).

In this paper, we report the isolation, amino acid sequencing, crystallization and three-dimensional structure determination of BEL. Similar to ABL, BEL is found to selectively inhibit the proliferation of several malignant cell lines. We also describe in detail the interactions of the lectin with specific mono- and disaccharides that can occupy the two distinct binding sites that are present in each protomer of the tetrameric protein.

## Results

### *Amino acid sequence of BEL*

Information on the amino acid sequence of BEL was obtained from three sources: Edman degradation and sequence analysis of the intact protein, cDNA sequencing of the gene encoding the lectin obtained from RNA extracts of the mushrooms and the X-ray high-resolution electron density maps. The sequence was also checked by tandem mass spectrometric analysis of the peptides derived from tryptic, chymotryptic and *S. Aureus* V8 endopeptidase cleavage. Supplementary material, Figure S1 summarizes the results obtained. Several positions in the polypeptide chain showed significant variability. The amino acids present in those positions are labeled in red in the figure. This variability, which was confirmed by all the methods used to gain information on the amino acid sequence, is probably due to the fact that the origin of all our samples was different commercial preparations, in every case labeled *B. edulis*, but which most likely contained different mixtures of hard to distinguish members of the genus *Boletus*.

The electron density map at 1.15 Å resolution of the native apoprotein was of sufficient quality to allow us to select one of the possible amino acids in the positions where variability was observed and that sequence was used for all the crystallographic work and for comparison of the BEL sequence with those of other mushrooms. BEL belongs to the saline-soluble family of mushroom fruiting body-specific lectins (Goldstein and Winter 2007; Singh et al. 2010). The proteins of this group have been described in the fruiting bodies of several well-known mushrooms. Figure 1 shows the BEL sequence aligned using the program CLUSTALW (Thompson et al. 1994) to the lectins present in *Xerocomus chrysenteron* (XCL; Trigueros et al. 2003), *Paxillus involutus* (PIL; Le Quere et al. 2006), *Sclerotium rolfsii* (SRL; Leonidas et al. 2007), ABL (Crenshaw et al. 1995) and *Pleurotus cornucopiae* (PCL; Iijima et al. 2002). BEL presents 82% amino acid identity with XCL, 66% with PIL, 58% with SRL, 57% with ABL and 52% with PCL. Similar proteins have been described in the fungi *Marchantia polymorpha* (Peumans et al. 2007), *Arthrobotrys oligospora* (Rosén, Bergström, et al. 1996; Rosén, Kata, et al. 1996), *Podospora anserina* (Paoletti and Saupe 2008) and *Neurospora crassa* (Hynes 2003).

A remarkable characteristic of these lectins is the presence of two distinct binding sites per protomer with different specificity, first described for the ABL (Carrizo et al. 2005). Some of the lectins in this group are tetramers, whereas others are believed to be dimers. All of our biochemical as well as crystallographic data are consistent with a tetrameric structure for BEL. The computed molecular mass of the protomer is 15,806 Da and the isoelectric point is 9.0, which is in reasonable agreement with our experimental observations.

### *Antiproliferative properties on carcinoma cell lines*

BEL exerts strong antiproliferative activity toward human carcinoma cell lines. The effect was measured *in vitro* as the inhibition of [$^3$H]-thymidine incorporation. In all of the cell lines, the inhibition showed lectin concentration dependence. Representative plots of percentage inhibition as a function of lectin concentration are shown in Figure 2. BEL produced a maximum effect of 92% against colon cancer cell line HT29 at a concentration of 10 µg/mL. At this concentration, the inhibition of liver cancer cell line HepG2 and breast cancer cell line Michigan Cancer Foundation (MCF)-7 was almost equal, 79 and 77%, respectively. The *in vitro* antiproliferative effect of BEL against human carcinoma cells in a dose-dependent manner is in consonance with the earlier reported antiproliferative activity of ABL (Yu et al. 1993). The reported maximum inhibitory effect of ABL against the HT29 cell line was of 87%, similar to that of BEL, but at a concentration of 25 µg/mL (at 10 µg/mL the inhibition was ∼80%). A more significant difference between BEL and ABL antiproliferative activities was observed against the MCF-7 cell line; in this case, the inhibitory effect of ABL was 50% at a concentration of 25 µg/mL.

### *X-ray structure of apo-BEL*

The tetramer of the proteins of this family has been described as a dimer of dimers (Carrizo et al. 2005). The orthorhombic crystals of the apo-crystal form of BEL contain, in the asymmetric unit, one protomer of each of the two dimers, the tetramer being generated by a crystallographic 2-fold axis (Figure 3). The final model of the protomers of the apoprotein contains 142 amino acids corresponding to 2240 protein atoms and 250 water molecules. The conventional *R* factor is 17.4% and the free *R* factor 18.8% (Table I). The *R* factors and root mean square deviations (r.m.s.d.) in Table I were calculated with the program REFMAC (Murshudov et al. 1997). The stereochemical quality of the protein model was assessed with the program PROCHECK (Laskowski et al. 1993). 93.0% of the residues are in the most favorable region of the

```
BEL                TYSITLRVFQRNPGRGFFSIVEKTVFHYANGGTWSEAKGTHTLTMGGSGTSGVLRFMSDK 60
XCL    Q8WZC9      SYSITLRVYQTNRDRGYFSIVEKTVWHFANGGTWSEANGAHTLTQGGSGTSGVLRFLSTK 60
PIL    Q5V8L0      SYSIKLRIHQPNIAGGFFSIVESTVWNYANGGTWSDADGNQTLTMGGSGTSGTLRFMSDS 60
SRL                TYKITVRVYQTNPN-AFFHPVEKTVWKYANGGTWTITDDQHVLTMGGSGTSGTLRFHADN 59
ABL    Q00022      TYTISIRVYQTTPK-GFFRPVERTNWKYANGGTWDEVRGEYVLTMGGSGTSGSLRFVSSD 59
PCL    Q96WQ6      SYTIKVRVFQTNPN-AFFRIVEQGVWHYANGGTWSDKDGVLTLTMGGSGTSGMLRFMTEQ 59

BEL                G-ELITVAVGVHNYKRWCDVVTGLKPEETALVINPQYYNN-GPRAYTREKQLAEYNVTSV 118
XCL    Q8WZC9      G-ERITVAVGVHNYKRWCDVVTGLKPDETALVINPQYYNN-GGRDYVREKQLAEYSVTSA 118
PIL    Q5V8L0      G-ERLIVAIGVHNYKRWCDIATGLAPNATGVVVNGEYYNS-GKRAYMREKQLSQYSVTSP 118
SRL                G-ESFTATFGVHNYKRWCDIVTNLAADETGMVINQQYYSQ-KNREEARERQLSNYEVKNA 117
ABL    Q00022      TDESFVATFGVHNYKRWCDIVTNLTNEQTALVINQEYYGV-PIRDQARENQLTSYNVANA 118
PCL    Q96WQ6      GKEAFFIAMGVHNYKRWVDIVTGLADDVTCVRALPEYYDDKSERARSREAQRITQSVLNI 119

BEL                VGTRFEVKYTVVEGNNLEANVIFS 142                                100%
XCL    Q8WZC9      IGTKVEVVYTVAEGNNLEANVIFS 142                                 82%
PIL    Q5V8L0      AGTKVAIKYTVADGNCLEADVTIG 142                                 66%
SRL                KGRNFEIVYTEAEGNDLHANLIIG 141                                 58%
ABL    Q00022      KGRRFAIEYTVTEGDNLKANLIIG 142                                 57%
PCL    Q96WQ6      DRRNISATYSVAEGNNLELNIVIG 143                                 52%
```

**Fig. 1.** Sequence comparison of fungal lectins. The sequences were aligned using the program CLUSTALW (Thompson et al. 1994) and correspond to the following lectins: BEL, *B. edulis* lectin; XCL, *X. chrysenteron* lectin; PIL, *P. involutus* lectin; SRL, *S. rolfsii* lectin; ABL, *A. bisporus* lectin; PCL, *P. cornucopiae* lectin. The residues conserved in all the members of the group are represented in red. The available ExPASy codes are indicated after the name of the lectin. The column on the right hand of the figure gives the percentage identity of each sequence with BEL. The green dots indicate the positions where there are variations in the BEL sequence (Supplementary material, Figure S1).

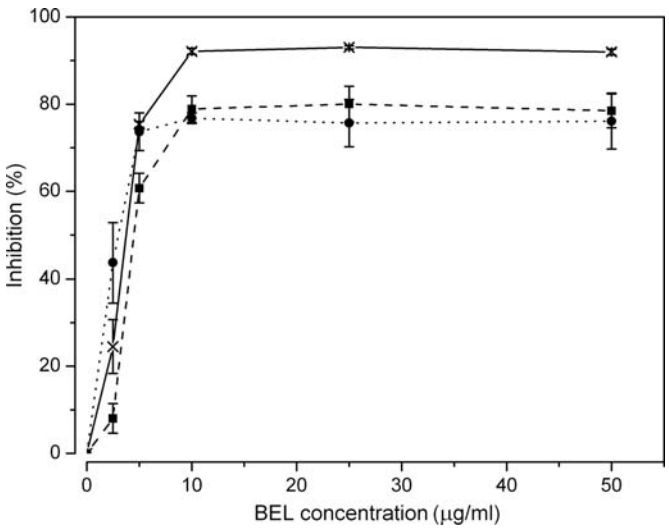


**Fig. 2.** Antineoplastic properties of BEL. BEL inhibition of [$^3$H]thymidine incorporation into DNA by tumor cell lines, HT29 (crosses), HepG2 (filled squares) and MCF-7 (filled circles). In the dose–response curves, the BEL effect is expressed as the percentage inhibition of the response obtained with the medium alone. The values plotted are the means ± SD of triplicate determinations.

Ramachandran plot and the remaining 7.0% in the additionally allowed region.

The overall fold of the BEL protomer is quite similar to that of ABL, i.e. it is a single domain structure organized as a β-sandwich (Figure 3) with six strands of β-chain in the first sheet (H, I, J, A, D, C) and four strands in the second (B, E, F, G). A helix-loop-helix motif, packed against the second sheet, connects the two sheets linking strand G to H. The secondary structure assignments are, for the β-strands, the following: strand A, residues 3–10; B, residues 18–25; C, residues 32–37; D, residues 40–45; E, residues 51–58; F, residues 63–71; G, residues 74–80; H, residues 112–116; I, residues 122–129; and J, residues 134–141. The two α-helices span residues 89–92 and 103–107. In addition, there are two $3_{10}$ helices spanning three residues, 13–15 and 28–30. The two dimers present in the asymmetric unit of the crystals of apo-BEL are very similar to each other, with an r.m.s.d. of 0.175 Å over 142 α-carbon atoms.

Three X-ray structures of members of this fungal lectin family are available: ABL, XCL and SRL. They are all very similar to BEL. The r.m.s.d. for the 142 α-carbons (in every case, protomers A in the PDB file were compared) are 2.296 Å for ABL (Carrizo et al. 2005, PDB code 1Y2T), 0.362 Å for XCL (Birck et al. 2004, PDB code 1XI0) and 3.676 Å for SRL (Leonidas et al. 2007, PDB code 2OFC; in this case, 141 α carbons were superimposed). Not surprisingly, the smallest differences are found with XCL, extracted from a mushroom of the same family, and with the highest sequence identity with BEL (Figure 1).

### *Lectin–carbohydrate interactions*

The two sugar-binding sites of the lectin are situated on the two sides of the helix-loop-helix motif. The GalNAc and T-antigen disaccharide-binding site (that we call binding site 1) in the shallow depression delimited by the loops

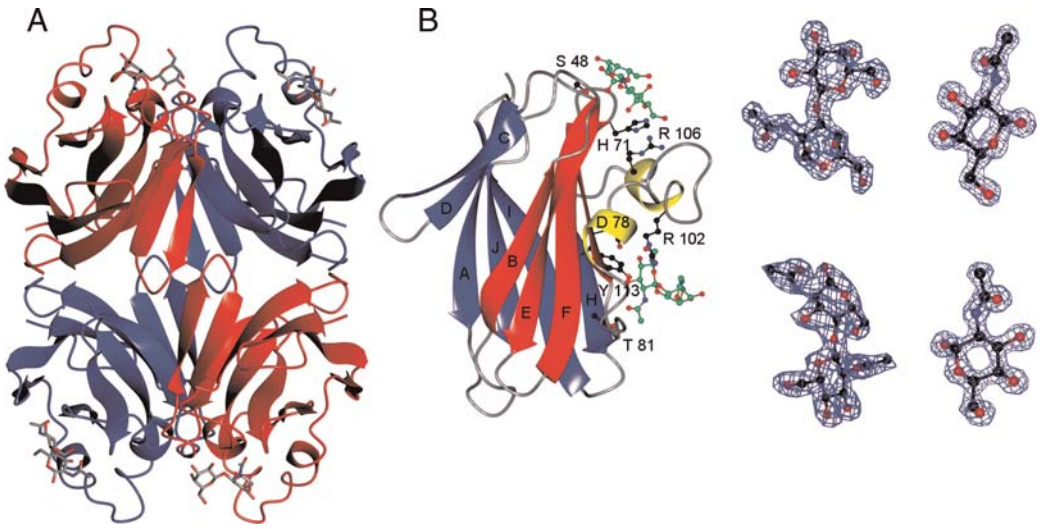


**Fig. 3.** X-ray structure of BEL. (**A**) Ribbon representation of the BEL tetramer with ball and stick models of the T-antigen disaccharide and *N*,*N*′-diacetylchitobiose. A crystallographic asymmetric unit is represented with protomers of the same color. The red protomers have the T-antigen disaccharide represented in binding site 1 and the blue protomers *N*,*N*′-diacetylchitobiose in binding site 2. The molecular tetramer has 222-point symmetry: two dyads intersecting in the center of the molecule are present in the plane of the figure, one horizontal and one vertical, the third is perpendicular to the plane. (**B**) Ribbon representation of the BEL protomer. The six stranded β-sheet is shown in blue and the four stranded sheet in red. The two short helices are in yellow and the connections are in gray. The two carbohydrates represented as ball and stick models are the T-antigen disaccharide (top) and *N*,*N*′-diacetylchitobiose (bottom). The electron densities closest to the model are those of the disaccharides in the crystals that contain only one disaccharide. The density on the right is that of a molecule of *N*-acetylgalactosamine (NGA) bound at the T-antigen binding site (top) and a molecule of *N*-acetylglucosamine (NAG) bound at the second binding site (bottom). The electron density of the 2Fobs-Fc maps corresponds to the ligands bound in the orthorhombic crystal form, and it was contoured at a 1.5 $\sigma$ level. The side chains of the main amino acids involved in the interactions are represented in the figure. The figure was prepared using the program CCP4mg (Potterton et al. 2002).

connecting strands B → C, D → E and F → G. The GlcNAc and *N*,*N*′-diacetylchitobiose (and most likely chitin)-binding site (that we call binding site 2) is delimited by residues from the last strand of the first β-sheet (G), the first strand of the second β-sheet (H) and the second of the two helices of the motif.

Table II lists the main contacts between the different carbohydrate molecules studied in the crystals and BEL. In every case, the protomer chosen to prepare the table was protomer A of the asymmetric unit. The table is divided into two parts to separate the two distinct binding sites. Note that the distances between the carbohydrates and the side chains are conserved in more than one crystal form (identified with the number between parenthesis used in the second row of Table I). They are also very similar in the different protomers present in the asymmetric units.

Binding of GalNAc is mediated by several hydrophobic interactions and the hydrogen bond established by its O7 and the OG of Ser48. At the other end of the sugar molecule, there are two important interactions between O6 and the NH2 of Arg106 and O5 and the NE2 of His71. Other hydrogen bonds are formed with the carbonyl of Gly49 and the N of Asn72.

In the second binding site, Asp78 is the key residue that confers specificity to binding of GlcNAc since its carboxylate oxygens make hydrogen bonds with O4 and O6 of the carbohydrate molecule. In addition, the OH of Tyr113 forms a hydrogen bond with O3 and the OG1 of Thr81 with O7.

Figure 4A is a stereo diagram showing the interaction of the T-antigen disaccharide and GalNAc with BEL at their common binding site (number 1). Figure 4B is a similar diagram with GlcNAc and *N*,*N*′-diacetylchitobiose at the second binding site (number 2). In Supplementary material, Figures S2 and S3 show on the left a ball and stick model of the sugars bound on the surface of the lectin molecule. The negatively charged residues are represented in red, the positively charged in blue and those with no charge in gray. The right-hand side of the figures is a scheme of the most important contacts.

The antiproliferative properties of ABL are known to be mediated through its binding to the Thomsen–Friedenreich antigen disaccharide (Galβ1-3GalNAc; Springer 1984, 1997), one of the few chemically well-defined antigens associated with neoplasia, suppressed in normal and exposed in malignant cells. Three different co-crystals of BEL and the T-antigen disaccharide were prepared one with the disaccharide alone and two in the presence of *N*,*N*′-diacetylchitobiose that occupies the second binding site. Figure 4A shows that the position of the GalNAc moiety of the T-antigen disaccharide overlaps very well with that of the monosaccharide and the BEL amino acid side chains participating in the contacts are the same. In addition, the distances between the atoms in contact are comparable (Table II). Two important contacts are also established with O2 and O4 of the galactose moiety of the T-antigen disaccharide and the O of Gly49 and the N of Ala29, respectively.

The electron density for the two *N*-acetylglucosamine moieties of *N*,*N*′-diacetylchitobiose is clearly defined only in the crystals that contain this disaccharide alone, whereas the co-crystals in the presence of the T-antigen disaccharide show defined electron density only for the *N*-acetylglucosamine part in closest contact with the BEL molecule. That moiety

**Table I.** Data collection and refinement statistics

| Data set | Apo-BEL | BEL + T-antigen | BEL + *N*,*N*′-diacetylchitobiose | BEL + NAG and NGA | BEL + NAG and NGA | BEL + T-antigen and *N*, *N*′-diacetylchitobiose | BEL + T-antigen and *N*, *N*′-diacetylchitobiose |
|---|---|---|---|---|---|---|---|
| Space group | $C222_1$ | $C222_1$ | $P2_12_12_1$ | $P6_122$ | $C222_1$ | $P6_122$ | $C222_1$ |
| Crystal form | 1 | 2 | 3 | 4 | 5 | 6 | 7 |
| *a* (Å) | 68.1 | 68.1 | 68.2 | 123.8 | 68.0 | 124.1 | 68.2 |
| *b* (Å) | 97.4 | 97.5 | 84.1 | 123.8 | 97.5 | 124.1 | 98.0 |
| *c* (Å) | 84.4 | 84.1 | 120.2 | 104.3 | 84.1 | 104.5 | 84.5 |
| $\alpha$ | 90.0 | 90.0 | 90.0 | 90.0 | 90.0 | 90.0 | 90.0 |
| $\beta$ | 90.0 | 90.0 | 90.0 | 90.0 | 90.0 | 90.0 | 90.0 |
| $\gamma$ | 90.0 | 90.0 | 90.0 | 120.0 | 90.0 | 120.0 | 90.0 |
| Protomers in the asymmetric unit | 2 | 2 | 4 | 2 | 2 | 2 | 2 |
| Resolution range (Å) | 29.3–1.15 | 33.6–1.30 | 39.7–2.00 | 45.0–1.90 | 33.6–1.30 | 29.3–2.00 | 48.97–1.70 |
| Observed reflections | 445,560 | 333,805 | 256,800 | 351,826 | 301,747 | 270,796 | 122,591 |
| Independent reflections | 95,942 | 66,455 | 47,335 | 36,987 | 67,738 | 32,555 | 31,154 |
| Multiplicity[a] | 4.6 (4.2) | 5.0 (3.9) | 5.4 (5.4) | 9.5 (9.4) | 4.5 (3.1) | 8.3 (7.9) | 3.9 (4.0) |
| Rmerge (%)[b] | 7.0 (17.7) | 5.2 (17.5) | 7.5 (24.3) | 6.9 (26.6) | 6.5 (19.5) | 7.1 (28.5) | 8.3 (32.2) |
| $<I/\sigma(I)>$ | 16.5 (6.9) | 19.5 (6.5) | 17.0 (6.3) | 21.9 (9.3) | 16.7 (4.3) | 19.9 (7.9) | 14.4 (5.1) |
| Completeness (%) | 96.8 (89.5) | 96.7 (81.0) | 99.9 (100.0) | 98.7 (99.6) | 98.5 (90.8) | 100.0 (100.0) | 99.3 (100.0) |
| Reflections in refinement | 91,124 | 63,017 | 44,892 | 35,136 | 64,211 | 30,853 | 29,554 |
| Rcryst. (%)[c] | 17.4 (19.1) | 17.0 (19.0) | 19.9 (23.2) | 17.8 (19.4) | 17.8 (21.4) | 19.2 (22.4) | 17.7 (25.9) |
| Rfree (%) (test set 5%)[d] | 18.8 (20.6) | 18.0 (20.7) | 24.0 (25.4) | 19.6 (22.0) | 19.1 (24.1) | 20.6 (23.9) | 20.8 (29.3) |
| Protein atoms | 2,240 | 2,240 | 4,480 | 2,240 | 2,240 | 2,240 | 2,240 |
| Ligand atoms | | 52 | 116 | 30 + 30 | 30 + 30 | 30 + 52 | 30 + 52 |
| Water molecules | 250 | 238 | 231 | 129 | 202 | 114 | 118 |
| r.m.s.d. on bond lengths (Å)[e] | 0.012 | 0.009 | 0.003 | 0.005 | 0.008 | 0.005 | 0.011 |
| r.m.s.d. on bond angles (°) | 1.479 | 1.293 | 0.731 | 0.919 | 1.178 | 0.815 | 1.226 |
| Planar groups (Å) | 0.009 | 0.007 | 0.003 | 0.007 | 0.006 | 0.003 | 0.006 |
| Chiral volume dev. ($Å^3$) | 0.099 | 0.084 | 0.049 | 0.080 | 0.077 | 0.055 | 0.092 |
| Average B factor ($Å^2$) | 9.4 | 9.0 | 21.6 | 22.0 | 9.7 | 22.5 | 11.7 |
| Protein atoms | 8.5 | 8.1 | 21.1 | 21.7 | 8.9 | 22.4 | 11.3 |
| Ligand atoms | | 11.0 | 35.7 | 32.5–20.7 | 10.1–11.4 | 20.1–28.7 | 17.5–12.0 |
| Solvent atoms | 17.4 | 17.4 | 23.1 | 24.4 | 17.3 | 23.3 | 18.5 |

[a]The values in parentheses refer to the highest resolution shells. For the data collection of apo-BEL, the highest resolution interval is 1.21–1.15 Å. For the other crystal forms, they are the following: 2, 1.37–1.30 Å; 3, 2.11–2.00 Å; 4, 2.00–1.90 Å; 5, 1.37–1.30 Å; 6, 2.11–2.00 Å; 7, 1.79–1.70 Å. The highest-resolution shells used in the refinements are the following: crystal form 1, 1.18–1.15 Å; 2, 1.33–1.30 Å; 3, 2.05–2.00 Å; 4, 1.95–1.90 Å; 5, 1.33–1.30 Å; 6, 2.05–2.00 Å; 7, 1.74–1.70 Å.

[b]Rmerge = $\Sigma h \Sigma i |I ih - <I h>| / \Sigma h \Sigma i <I h>$, where $<I h>$ is the mean intensity of the *i* observations of reflection *h*.

[c]Rcryst = $\Sigma ||Fobs| - |Fcalc|| / \Sigma |Fobs|$, where |Fobs| and |Fcalc| are the observed and the calculated structure factor amplitudes, respectively. Summation includes all reflections used in the refinement.

[d]Rfree = $\Sigma ||Fobs| - |Fcalc|| / \Sigma |Fobs|$, evaluated for a randomly chosen subset of 5% of the diffraction data not included in the refinement.

[e]Root mean square deviation from ideal values.

superimposes well with the GlcNAc molecule bound in the co-crystals with the monosaccharides, and the BEL residues that participate in sugar binding are the same (Table II). The second *N*-acetylglucosamine part of the disaccharide is in contact with Val80 and Arg102.

## Discussion

Exploiting its affinity for chitin, a new lectin was isolated from the fruiting bodies of the widely diffused wild edible mushroom *B. edulis*. The protein belongs to the saline soluble family of mushroom lectins and is structurally closely related to XCL and ABL.

Recently, a lectin with mitogenic activity was isolated with conventional biochemical methods from the fruiting bodies of *B. edulis* (Zheng et al. 2007). It was reported to be similar to ABL, to be specific for melibiose and xylose and to have the following N-terminus amino acid sequence: TYGIALRW. Although the protein protomer has a molecular weight which is similar to that of BEL, it appears to be a dimer and not a tetramer and therefore, considering also the differences in amino acid sequence of the short stretch available, it is probably not BEL.

The three-dimensional structure of three lectins similar to BEL is known: ABL, XCL and SRL. Extensive crystallographic data are available on co-crystals of ABL with mono- and disaccharides and SRL co-crystals with GalNAc and GlcNAc.

**Table II.** Selected distances between the closest BEL residues (in every case protomer A of the asymmetric unit) and the different carbohydrates

| BEL residue | Atom | Carbohydrate molecule | Atom | Distance (Å) (crystal form) | Distance (Å) (crystal form) | Distance (Å) (crystal form) |
|---|---|---|---|---|---|---|
| Binding site 1 (T-antigen) | | | | | | |
| Ala29 | N | T-antigen disaccharide | O4 (GAL) | 2.9 (2) | 2.9 (6) | 2.9 (7) |
| Ser48 | OG | T-antigen disaccharide | O7 (NGA) | 2.6 (2) | 2.8 (6) | 2.6 (7) |
| Ser48 | O | T-antigen disaccharide | O2 (GAL) | 2.7 (2) | 2.7 (6) | 2.7 (7) |
| Gly49 | O | T-antigen disaccharide | O4 (NGA) | 2.7 (2) | 2.7 (6) | 2.7 (7) |
| His71 | NE2 | T-antigen disaccharide | O5 (NGA) | 3.3 (2) | 3.6 (6) | 3.4 (7) |
| Asn72 | N | T-antigen disaccharide | O7 (NGA) | 2.8 (2) | 2.9 (6) | 2.8 (7) |
| Arg106 | NH2 | T-antigen disaccharide | O6 (NGA) | 3.4 (2) | 3.5 (6) | 3.4 (7) |
| Ser48 | OG | GalNAc | O7 | 2.7 (4) | 2.7 (5) | |
| Gly49 | O | GalNAc | O4 | 2.7 (4) | 2.8 (5) | |
| His71 | NE2 | GalNAc | O5 | 3.5 (4) | 3.3 (5) | |
| Asn72 | N | GalNAc | O7 | 2.9 (4) | 2.8 (5) | |
| Arg106 | NH2 | GalNAc | O6 | 3.5 (4) | 3.3 (5) | |
| Binding site 2 (*N*,*N*′-diacetylchitobiose) | | | | | | |
| Asp78 | OD1 | *N*,*N*′-diacetylchitobiose | O6 (144) | 2.7 (3) | 2.7 (6) | 2.7 (7) |
| Asp78 | OD2 | *N*,*N*′-diacetylchitobiose | O4 (144) | 2.6 (3) | 2.6 (6) | 2.7 (7) |
| Val79 | O | *N*,*N*′-diacetylchitobiose | O3 (144) | 2.6 (3) | 2.7 (6) | 2.7 (7) |
| Thr81 | OG1 | *N*,*N*′-diacetylchitobiose | O7 (144) | 2.8 (3) | 2.8 (6) | 2.7 (7) |
| Arg102 | NH1 | *N*,*N*′-diacetylchitobiose | O6 (144) | 3.0 (3) | 2.9 (6) | 2.9 (7) |
| Tyr113 | OH | *N*,*N*′-diacetylchitobiose | O3 (144) | 2.6 (3) | 2.6 (6) | 2.7 (7) |
| Asp78 | OD1 | GlcNAc | O6 | 2.7 (4) | 2.7 (5) | |
| Asp78 | OD2 | GlcNAc | O4 | 2.7 (4) | 2.6 (5) | |
| Val79 | O | GlcNAc | O3 | 2.7 (4) | 2.8 (5) | |
| Thr81 | OG1 | GlcNAc | O7 | 2.8 (4) | 2.7 (5) | |
| Arg102 | NH1 | GlcNAc | O6 | 2.7 (4) | 2.9 (5) | |
| Tyr113 | OH | GlcNAc | O3 | 2.6 (4) | 2.7 (5) | |

The notation used for the T-antigen disaccharide kept the numbering of the two independent monosaccharides: GAL, galactose; NGA, *N*-acetylgalactosamine. The two monomers of *N*,*N*′-diacetylchitobiose were labeled 144 and 145 and are clearly visible only in the orthorhombic crystal form with *N*,*N*′-diacetylchitobiose alone ($P2_12_12_1$), although the main contacts listed in the table are with only one of the monomers.

Binding of GalNAc in binding site 1 in both ABL and SRL is very similar to the binding of the monosaccharide in BEL, and all of the amino acids involved in the important contacts listed in Table II are conserved in the three proteins.

Comparison of this binding site with that of another fungal lectin, galectin GCL2 from the inky cup mushroom *Coprinopsis cinerea* (Walser et al. 2004, PDB code 1ULG) reveals that whereas in BEL it is the GalNAc moiety of the T-antigen disaccharide that is in closest contact with the lectin, in GCL2 it is the Gal part of the disaccharide that is in more intimate contact with the protein. Figure 5A and B compares the binding of the T-antigen disaccharide to the two fungal lectins.

Since this is the first X-ray structure of a complex of a saline soluble mushroom lectin and *N*,*N*′-diacetylchitobiose, no comparison with another member of this lectin family is possible. As evidenced from the distances in Table II, most of the important interactions are established with one of the GlcNAc moieties of the disaccharide and the contacts are similar to those observed for the monosaccharide alone. Figure 5C and D compares the binding of *N*,*N*′-diacetylchitobiose to BEL and that of chitotetraose of the fungal lectin CGL3 in the mushroom *C. cinerea* (Wälti et al. 2008, PDB code 2R0H). In the case of CGL3, important contacts are observed with all the three monosaccharide units for which electron density is clear in the maps.

This second BEL-binding site contains most likely the amino acids that bind chitin during the purification protocol of the protein but the fact that the contacts are established mostly with only one monosaccharide unit coupled to the observation that the second sugar monomer is disordered in two out of the three crystal forms containing *N*,*N*′-diacetylchitobiose suggests that, if a physiological interaction with chitin exists, it is probably rather weak. If that interaction exists *in vivo* and the lectin is bound to the chitin-containing cell wall, one might suggest that the role of the T-antigen disaccharide-binding site might be to link the cell wall to the host for adhesion, a process that is often achieved through the binding of a fungal lectin to a host glycoprotein.

## Materials and methods

### *Protein purification*

Two purification methods were used to isolate the protein; the first exploited the binding of the lectin to a chitin column, whereas the second was a modification of a method originally proposed for the purification of the ABL (Betail et al. 1975).

In each preparation, ~500 g of king bolete mushrooms was homogenized in a blender for 3 min at 4°C using approximately the same volume of 50 mM Tris–HCl, pH 7.5, 1 mM $CaCl_2$, 1 mM $MgCl_2$, 0.15 M NaCl, 0.02% $NaN_3$. After filtering through glass wool, the suspension was centrifuged at 14.300 g at 4°C for 30 min and the precipitate discarded. The supernatant was loaded onto a 20 mL chitin column previously equilibrated with the buffer used to homogenize the mushrooms, and the column was washed until the absorbance of the effluent at 280 nm was negligible.

The bound lectin was then eluted by adding 0.25 M *N*-acetylglucosamine to the initial Tris buffer, dialyzed exhaustively, concentrated and submitted to gel filtration

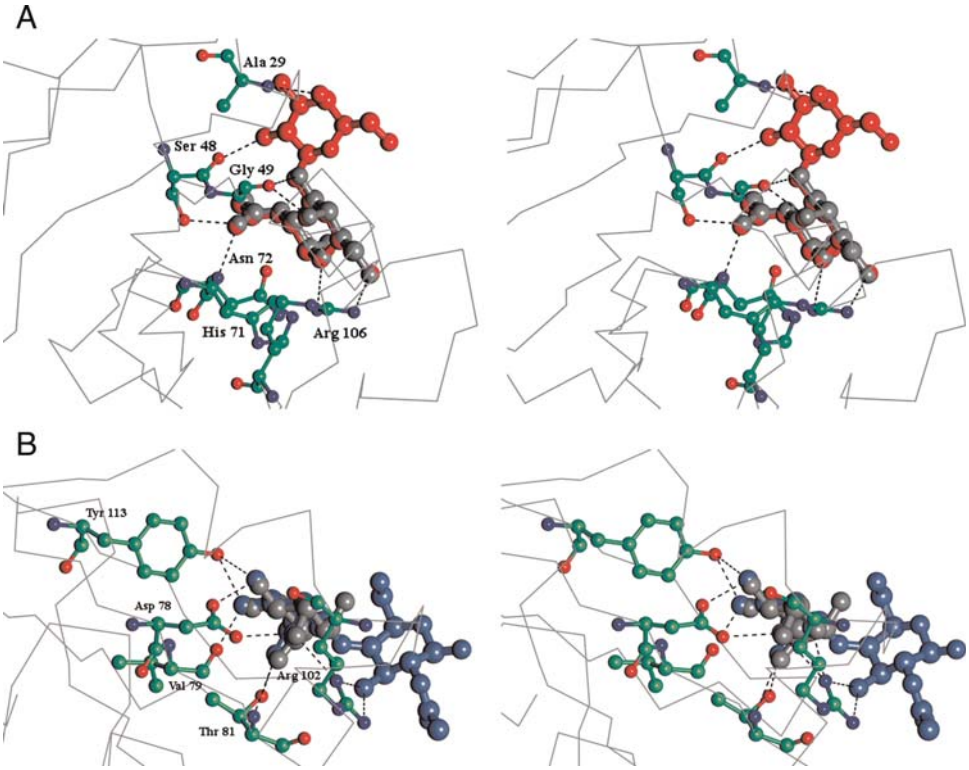


**Fig. 4.** Binding of carbohydrates to BEL. (**A**) Stereo representation of BEL-binding site 1 (T-antigen disaccharide) with the T-antigen disaccharide (red) and N-acetylgalactosamine (gray) and important BEL side chains involved in the interactions represented as ball and stick models. Hydrogen bonds are represented as dashed lines. (**B**) Stereo representation of BEL-binding site 2 (*N*,*N*′-diacetylchitobiose) with *N*,*N*′-diacetylchitobiose (blue) and N-acetylglucosamine (gray) The figure was prepared using the program CCP4mg (Potterton et al. 2002).

chromatography using a Superdex G-200 column HR 10/30 (GE Healthcare, Piscataway, NJ, USA).

The final purification step used the Lipidex 1000 resin, and the hydrophobic interaction chromatography was performed in a column thermostated at 37°C. The yield was ~10–15 mg of protein for 500 g of starting material.

In the second purification method, the mushrooms were homogenized in saline and the filtered solution applied to a 200 mL column of human erythrocytic stroma incorporated into a polyacrylamide gel (Betail et al. 1975). After extensive washing to remove all the unbound protein, the lectin was recovered by adding 0.1 M ammonia to the saline used for elution. The gel filtration and hydrophobic interaction chromatography steps were identical to those used in the alternative method. The advantage of this second method was that the purified protein had not been in contact with *N*-acetylglucosamine; its disadvantage was that it contained significant amounts of a second lectin that had to be eliminated before using. The mixtures of the two lectins were dialyzed against 20 mM Tris–HCl, pH 8.0, loaded onto a MiniQ™ PE 4.6/50 column (GE Healthcare) equilibrated in the same buffer and resolved using an Äkta UPC900 chromatographic system (GE Healthcare). Under these conditions, BEL did not bind to the column whereas the other lectin did. The protein purified with both methods showed one band in Sodium dodecyl sulfate polyacrylamide gel electrophoresis. More details on this second purification method are given in the Supplementary material.

*Amino acid sequence determination*

Automated Edman degradation and sequence analysis of the native purified BEL (1.0 nmol) were performed on a Hewlett-Packard model G 1000A (Palo Alto, Ca, USA) sequencer connected online to a phenylthiohydantoin analyzer from the same manufacturer.

For proteolytic digestion, BEL aliquots (50 µg) were dissolved in 100 µL of 100 mM ammonium bicarbonate, pH 8.5, and reduced for 20 min at 56°C with 1 mM dithiothreitol. Proteolysis was performed with either endopeptidase V8 from *S. Aureus* (Sigma-Aldrich, St Louis, MO, USA), trypsin (Trypsin Gold, Promega, Fitchburg, WI, USA) or chymotrypsin (sequencing grade, Promega). For trypsin and chymotrypsin digestions, the reaction was performed at 37°C for 2 h, adding 1.8 µg of proteases and 0.01% (v/v) ProteaseMAX™ Surfactant (Promega). V8 digestion used 2 µg of enzyme at 37°C for 4 h. In all cases, the reaction was stopped by the addition of 1% (v/v) formic acid.

Peptides were resolved in an analytical Jupiter $C_{18}$ column (4 µm, 150 × 2 mm, Phenomenex, Torrance, CA, USA) at a flow rate of 0.2 mL/min with a gradient 3–70% B in 90 min, 70–97% B in 5 min and 98% B in 10 min. The solvents were water (A) and acetonitrile (B) both containing 0.1% formic acid. The eluent was analyzed online with an LCQ ion trap mass spectrometer (Thermo Fisher Scientific, Waltham, MA USA) with ESI ion source controlled by the Xcalibur software 1.4 (Thermo Scientific). Mass spectra were generated in

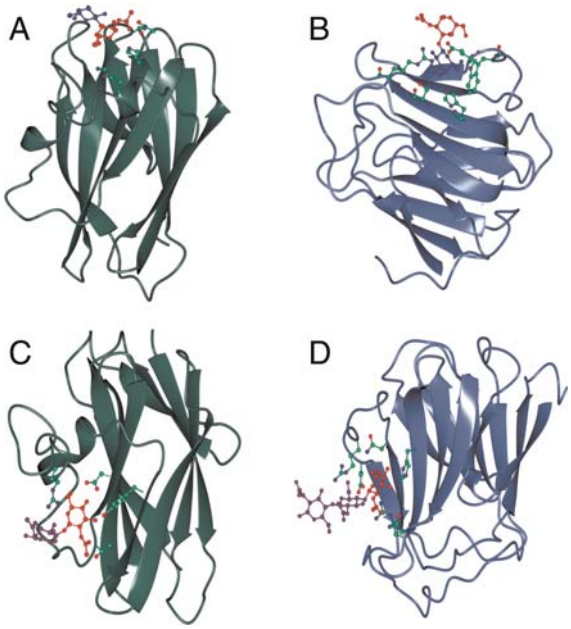


**Fig. 5.** Comparison of saccharide binding to BEL and other fungal lectins. The panels on the left (**A** and **C**) represent the BEL protomer (green) with the T-antigen disaccharide (A) and *N*,*N*′-diacetylchitobiose (C) drawn as ball and stick models. The panels on the right represent the *C. cinerea* GCL2 lectin (**B**) and the *C. cinerea* GCL3 lectin (**D**). The contacts of BEL and the T-antigen disaccharide are established with the GalNAc moiety (red), whereas those of the T-antigen disaccharide with GCL2 involve the galactose (blue) moiety. The *C. cinerea* GCL3 lectin (D) is complexed with chitotetraose but only three monomers are present in the model. The BEL contacts with *N*,*N*′-diacetylchitobiose are mostly with the non-reducing end of the disaccharide (red), whereas those of the trisaccharide and GCL3 involve atoms from the three sugar monomers.

positive ion mode under constant instrumental conditions. Mass spectrometry (MS)/MS spectra, obtained by collision-induced dissociation in the linear ion trap, were recorded with a resolution of 3 Da (*m*/*z*), the activation amplitude was 35% of ejection radio frequency amplitude that corresponds to 1.58 V. Tandem mass spectra were automatically analyzed using Peaks Studio, version 5.2 (Bioinformatic Solution Inc., Waterloo, ON, Canada) and also interpreted manually with the assistance of the prediction algorithm for peptide fragmentation ProteinProspector (Clauser et al. 1999).

In addition, trypsin and chymotrypsin in gel digestions were performed. Protein bands were excised from the gel and washed in 50 mM ammonium bicarbonate, pH 8.0, followed by a 50% acetonitrile solution until complete destaining. The gel bands were dried under vacuum, resuspended in 50 mM ammonium bicarbonate, pH 8.0, 0.01% ProteaseMAX™ Surfactant, 0.25 µg of trypsin or chymotrypsin and digested at 37°C for 2 h. The reaction was stopped by the addition of 1% (v/v) formic acid, and after centrifugation, the supernatant was analyzed by liquid chromatography-electro spray ionisation-MS/MS.

Total RNA was isolated from commercial fruiting bodies using Trizol Reagent (Invitrogen, Carlsbad, CA, USA) according to the manufacturer's protocol. The RNA was treated with RQ1 RNase-Free DNase (Promega) to remove contaminating DNA. The first-strand cDNA was synthesized from the total mushroom RNA using an oligo-dT primer and SuperScript Reverse Transcriptase II (Invitrogen). The BEL cDNA was amplified using 5′- and 3′-degenerated primers designed on the basis of the amino acid sequence of the N- and C-terminal portions of the protein. The amplified band was purified in a 1% agarose gel and cloned into the pGEM-T Easy vector for sequencing.

### *Cell proliferation assays*

The human colonic adenocarcinoma HT29 cell line, human mammary adenocarcinoma MCF-7 cell line and hepatocellular carcinoma HepG2 cell line were obtained from the American Type Culture Collection (ATCC, Manassas ,VA, USA). Cells were grown and maintained at 37°C in 5% $CO_2$ in Dulbecco's modified Eagle's medium (DMEM) supplemented with 5% fetal bovine serum, 100 µg/mL of penicillin and 100 µg/mL of streptomycin.

For the proliferation assays (Yu et al. 1993), cells were seeded at a density of $1.5 \times 10^4$/well in 0.5 mL of DMEM containing 5% fetal bovine serum in 24-well plates. After 48 h incubation at 37°C in 5% $CO_2$, the growth medium of each well was replaced by 0.5 mL of DMEM containing 250 µg/mL of bovine serum albumin. The cells were incubated at 37°C for 24 h in this medium. After the addition of the lectin, the cells were incubated for a further 24 h prior to a 1 h pulse with 0.5 µCi/well [methyl-$^3$H]-thymidine. In the subsequent step, the cells were washed twice with phosphate-buffered saline and precipitated by addition of 0.5 mL/well of 5% trichloroacetic acid at 4°C. After two washes with 0.5 mL/well of 95% ethanol at 4°C, the precipitate was solubilized with 0.5 mL/well of 0.2 M NaOH. The dissolved precipitate was mixed with scintillation solution, and the cell-associated radioactivity was counted using a liquid-scintillation spectrometer.

### *Crystallization, X-ray data collection, structure solution and refinement*

The purified protein was dialyzed against either 50 mM Tris–HCl, pH 7.5, or saline, concentrated to 20 mg/mL and used at this concentration for the initial screen of crystallization conditions. Molecular Dimensions Structure Screens (Newmarket, Suffolk, UK) were used at 20°C with the hanging-drop method, mixing 1 µL of the protein solution with the same volume of the precipitating solution and equilibrating against a volume of 0.3 mL of the latter in the reservoir. The conditions yielding small crystals were later refined, and the sitting-drop method with larger volumes was also tested until crystals that were large enough for data collection were obtained.

Three different crystal forms were obtained. The first crystal form in the presence of *N*-acetylglucosamine using as precipitant 0.2 M ammonium acetate, 0.1 M sodium acetate, pH 4.6, 30% PEG 4000. These crystals are hexagonal, space group $P6_122$ with $a = b = 123.8$ Å and $c = 104.3$ Å. They can be soaked in solutions containing both *N*-acetylglucosamine and *N*-acetylgalactosamine or in solutions containing the T-antigen and *N*,*N*′-diacetylchitobiose that displaces the bound monosaccharide. The second crystal form was obtained in the presence of *N*,*N*′-diacetylchitobiose and the following precipitating

solution: 0.2 M magnesium acetate, 0.1 M sodium cacodylate, pH 6.5, 10% PEG 8000. The crystals are orthorhombic, space group $P2_12_12_1$ with $a = 68.2$ Å, $b = 84.1$ Å and $c = 120.2$ Å. Finally, the apoprotein crystals grow in 1.6 M ammonium sulfate, 10% dioxane, 0.05 M 4-morpholineethanesulfonic aci, pH 6.5. The same crystal form can be obtained in the presence of both *N*-acetylglucosamine and *N*-acetylgalactosamine or in solutions containing *N*,*N*′-diacetylchitobiose. These crystals are also orthorhombic but the space group is $C222_1$ with $a = 68.1$ Å, $b = 97.4$ Å and $c = 84.4$ Å. The crystals containing the monosaccharides could be prepared both by co-crystallization and soaking and were indistinguishable. The data used for the final refinement were collected from crystals prepared by co-crystallization. The crystals containing the disaccharides were prepared only by soaking. In every case, the carbohydrate concentration used was ~20 mM. Soaking experiments using different combinations of carbohydrates were carried out, and the two sites were found completely independent.

The data were collected at different beamlines of the European Synchrotron Radiation Facility in Grenoble, at 100° K after a brief soaking in a mixture of 80% of the mother liquor and 20% glycerol. These data were indexed, integrated and reduced using the programs MOSFLM and Scala (Leslie 1992; Collaborative Computational Project Number 4 1994). The diffraction data statistics are summarized in Table I.

The structure of the hexagonal crystal form was solved first using the CCP4 suite of programs for crystallographic computing. The initial phases were calculated by the molecular replacement method as implemented in the program MOLREP (Vagin and Teplyakov 2000), with the coordinates of a protomer of ABL (Carrizo et al. 2005; Protein data bank accession code 1Y2T) as the search probe. The automatic search with data up to a resolution of 3.0 Å gave a rotation function with two peaks that were significantly higher than all the others with Rf/sigma equal to 6.56 and 6.01. The third peak had an Rf/sigma of 3.97. The correlation coefficient of the dimer was 52.3 and the initial *R* factor of 55.8%. The model was rigid body refined using the program REFMAC (Murshudov et al. 1997) moving initially the entire dimer, and in a second stage, the two protomers and, at this point the *R* factor, dropped to 46.4%. After the proper side chains had been introduced, the model was subjected to a series of rounds of positional refinement alternated with manual model revisions with the program Coot (Emsley et al. 2010) and the refinement program REFMAC. During the process of refinement and model building, the quality of the model was controlled with the program PROCHECK (Laskowski et al. 1993). Ligands and solvent molecules were added to the model in the final stages of refinement, the latter according to the hydrogen-bond criteria and only if their *B* factors refined to reasonable values and if they improved the Rfree.

A similar procedure was followed to solve and refine the structure of the complex with *N*,*N*′-diacetylchitobiose that crystallizes in the space group $P2_12_12_1$ but in this case the molecular replacement program used was AMoRe (Navaza 1994) and the search probe was a BEL tetramer. There was a single very clear solution for both the rotation and translation functions calculated to a resolution of 3.0 Å. After fitting the correlation coefficient was 73.7 and the *R* factor of 37.8%. The other orthorhombic crystal form, space group $C222_1$, was solved using again the program MOLREP with a BEL protomer as the search probe. After rigid body refinement the model, which contains two protomers in the asymmetric unit, had a correlation coefficient of 44.4 and an *R* factor of 45.2%.

Refinement of these structures was also carried out with the program REFMAC following essentially the same procedure described for the hexagonal crystal form. The final refinement statistics for the models of the three crystal forms are summarized in Table I.

## Supplementary data

Supplementary data for this article is available online at http://glycob.oxfordjournals.org/.

## Acknowledgements

We are grateful to the staff of the ESRF in Grenoble (Proposal MX 805) for assistance during data collection. The coordinates of the models and the structure factors of the apoprotein and the complexes with carbohydrates have been deposited in the protein data bank; accession codes 3QDS, 3QDT, 3QDU, 3QDV, 3QDW, 3QDX and 3QDY.

## Funding

This work was supported by a FIRB (Fondo per gli Investimenti della Ricerca di Base) grant from the Italian Ministry of the Universities and Scientific Research. M.B. is supported by Fondazione Cassa di Risparmio di Verona, Vicenza, Belluno e Ancona.

## Conflict of interest

None declared.

## Abbreviations

ABL, *Agaricus bisporus* lectin; BEL, *Boletus edulis* lectin; DMEM, Dulbecco's modified Eagle's medium; GalNAc, *N*-acetylgalactosamine; GlcNAc, *N*-acetylglucosamine; NAG, *N*-acetylglucosamine; NGA, *N*-acetylgalactosamine; T-antigen, Thomsen–Friedenreich antigen; Galβ1-3GalNAc, Thomsen–Friedenreich disaccharide.

## References

Betail G, Coulet M, Genaud L, Guillot J, Scandariato M. 1975. Erythrocyte stroma included in polyacrylamide gel. Applications to affinity chromatography. *C R Séances Soc Biol Fil*. 169:561–566.

Birck C, Damian L, Marty-Detraves C, Lougarre A, Schulze-Briese C, Koehl P, Fournier D, Paquereau L, Samama JP. 2004. A new lectin family with structure similarity to actinoporins revealed by the crystal structure of *Xerocomus chrysenteron* lectin XCL. *J Mol Biol*. 344:1409–1420.

Carrizo ME, Capaldi S, Perduca M, Irazoqui FJ, Nores GA, Monaco HL. 2005. The antineoplastic lectin of the common edible mushroom (*Agaricus bisporus*) has two binding sites, each specific for a different configuration at a single epimeric hydroxyl. *J Biol Chem*. 280:10614–10623.

Clauser KR, Baker PR, Burlingame AL. 1999. Role of accurate mass measurement (±10 ppm) in protein identification strategies employing MS or MS/MS and database searching. *Anal Chem*. 71:2871–2882.

Collaborative Computational Project Number 4. 1994. *Acta Cryst*. D50:760—767.
Crenshaw RW, Harper SN, Moyer M, Privalle LS. 1995. Isolation and characterization of a cDNA clone encoding a lectin gene from *Agaricus bisporus*. *Plant Physiol*. 107:1465–1466.
Emsley P, Lohkamp B, Scott WG, Cowtan K. 2010. Features and development of *Coot*. *Acta Crystallogr D Biol Crystallogr*. 66:486–501.
Goldstein IJ, Winter HC. 2007. Mushroom lectins. In: Kamerling JP, editor. *Comprehensive Glycoscience: From Chemistry to Systems Biology*, Vol. 3. Amsterdam: Elsevier Ltd. p. 601–621.
Gonzàlez De Mejia E, Prisecaru VI. 2005. Lectins as bioactive plant proteins: A potential in cancer treatment. *Crit Rev Food Sci Nutr*. 45:425–445.
Hall IR, Lyon JE, Wang Y, Sinclair L. 1998. Ectomycorrhizal fungi with edible fruiting bodies 2. *Boletus edulis*. *Economic Botany*. 52:44–56.
Hall IR, Yun W, Amicucci A. 2003. Cultivation of edible ectomycorrhizal mushrooms. *Trends Biotechnol*. 21:433–438.
Hynes MJ. 2003. The *Neurospora crassa* genome opens up the world of filamentous fungi. *Genome Bio*. 4:217.
Iijima N, Yoshino H, Ten LC, Ando A, Watanabe K, Nagata Y. 2002. Two genes encoding fruit body lectins of *Pleurotus cornucopiae*: Sequence similarity with the lectin of a nematode-trapping fungus. *Biosci Biotechnol Biochem*. 66:2083–2089.
Imberty A, Mitchell EP, Wimmerová M. 2005. Structural basis of high-affinity glycan recognition by bacterial and fungal lectins. *Curr Opin Struct Biol*. 15:525–534.
Kabsch W. 1978. A solution for the best rotation to relate two sets of vectors. *Acta Cryst*. A32:922–923.
Khan F, Khan MI. 2011. Fungal lectins: Current molecular and biochemical perspectives. *Int J Biol Chem*. 5:1–20.
Laskowski RA, MacArthur MW, Moss DS, Thornton JM. 1993. PROCHECK: A program to check the stereochemical quality of protein structures. *J Appl Crystallogr*. 26:283–291.
Leonidas DD, Swamy BM, Hatzopoulos GN, Gonchigar SJ, Chachadi VB, Inamdar SR, Zographos SE, Oikonomakos NG. 2007. Structural basis for the carbohydrate recognition of the *Sclerotium rolfsii* lectin. *J Mol Biol*. 368:1145–1161.
Le Quere A, Eriksen KA, Rajashekar B, Schutzendubel A, Canback B, Johansson T, Tunlid A. 2006. Screening for rapidly evolving genes in the ectomycorrhizal fungus *Paxillus involutus* using cDNA microarrays. *Mol Ecol*. 15:535–550.
Leslie AGW. 1992. Recent changes to the MOSFLM package for processing film and image plate data. *Jnt CCP4/ESF-EACMB Newslett Protein Crystallogr*. 26:27–33.
Murshudov GN, Vagin AA, Dodson EJ. 1997. Refinement of macromolecular structures by the maximum-likelihood method. *Acta Crystallogr D Biol Crystallogr*. 53:240–255.
Navaza J. 1994. AMoRe: An automated package for molecular replacement. *Acta Crystallogr*. A5:157–163.
Paoletti M, Saupe SJ. 2008. The genome sequence of *Podospora anserina*, a classic model fungus. *Genome Biol*. 9:223.
Peumans WJ, Fouquaert E, Jauneau A, Rougé P, Lannoo N, Hamada H, Alvarez R, Devreese B, Van Damme EJ. 2007. The liverwort *Marchantia polymorpha* expresses orthologs of the fungal *Agaricus bisporus* agglutinin family. *Plant Physiol*. 144:637–647.
Potterton E, McNicholas S, Krissinel E, Cowtan K, Noble M. 2002. The *CCP4* molecular-graphics project. *Acta Crystallogr D Biol Crystallogr*. 58:1955–1957.
Reisner Y, Itzicovitch L, Meshorer A, Sharon N. 1978. Hemopoietic stem cell transplantation using mouse bone marrow and spleen cells fractionated by lectins. *Proc Natl Acad Sci USA*. 75:2933–2936.
Rosén S, Bergström J, Karlsson KA, Tunlid A. 1996. A multispecific saline-soluble lectin from the parasitic fungus *Arthrobotrys oligospora*. Similarities in the binding specificities compared with a lectin from the mushroom *Agaricus bisporus*. *Eur J Biochem*. 238:830–837.
Rosén S, Kata M, Persson Y, Lipniunas PH, Wikstrom M, Van Den Hondel MJ, Van Den Brink J, Rask L, Heden LO, Tunlid A. 1996. Molecular characterization of a saline-soluble lectin from a parasitic fungus. Extensive sequence similarities between fungal lectins. *Eur. J. Biochem*. 238:822–829.
Sharon N. 2006. Carbohydrates as future anti-adhesion drugs for infectious diseases. *Biochim Biophys Acta*. 1760:527–537.
Sharon N. 2007. Lectins: Carbohydrate-specific reagents and biological recognition molecules. *J Biol Chem*. 282:2753–2764.
Sharon N, Lis H. 2004. History of lectins: From hemagglutinins to biological recognition molecules. *Glycobiology*. 14:53R–62R.
Singh RS, Bhari R, Kaur HP. 2010. Mushroom lectins: Current status and future perspectives. *Crit Rev Biotechnol*. 30:99–126.
Springer GF. 1984. T and Tn, general carcinoma autoantigens. *Science*. 224:1198–1206.
Springer GF. 1997. Immunoreactive T and Tn epitopes in cancer diagnosis, prognosis, and immunotherapy. *J Mol Med*. 75:594–602.
Taylor AFS, Alexander I. 2005. The ectomycorrhizal symbiosis: Life in the real world. *Mycologist*. 19:102–112.
Thompson JD, Higgins DG, Gibson TJ. 1994. CLUSTAL W: Improving the sensitivity of progressive multiple sequence alignment through sequence weighting, position-specific gap penalties and weight matrix choice. *Nucleic Acids Res*. 22:4673–4680.
Trigueros V, Lougarre A, Ali-Ahmed D, Rahbe Y, Guillot J, Chavant L, Fournier D, Paquereau L. 2003. *Xerocomus chrysenteron* lectin: Identification of a new pesticidal protein. *Biochim Biophys Acta*. 1621:292–298.
Vagin A, Teplyakov A. 2000. An approach to multi-copy search in molecular replacement. *Acta Crystallogr D Biol Crystallogr*. 56: 1622–1624.
Wallace AC, Laskowski RA, Thornton JM. 1995. LIGPLOT: A program to generate schematic diagrams of protein-ligand interactions. *Protein Eng*. 8:127–134.
Walser PJ, Haebel PW, Künzler M, Sargent D, Kües U, Aebi M, Ban N. 2004. Structure and functional analysis of the fungal galectin CGL2. *Structure*. 12:689–702.
Wälti MA, Walser PJ, Thore S, Grünler A, Bednar M, Künzler M, Aebi M. 2008. Structural basis for chitotetraose coordination by CGL3, a novel galectin-related protein from *Coprinopsis cinerea*. *J Mol Biol*. 379: 146–59.
Wellens A, Garofalo C, Nguyen H, Van Gerven N, Slättegård R, Hernalsteens J, Wyns L, Oscarson S, Greve H, Hultgren S, et al. 2008. Intervening with urinary tract infections using anti-adhesives based on the crystal structure of the FimH-oligomannose-3 complex. *PLoS One*. 3:e2040.
Wu T, Zivanovic S, Draughon FA, Sams CE. 2004. Chitin and chitosan—value-added products from mushroom waste. *J Agric Food Chem*. 52:7905–7910.
Yu LG. 2007. The oncofetal Thomsen–Friedenreich carbohydrate antigen in cancer progression. *Glycoconj J*. 24:411–420.
Yu L-G, Fernig DG, Rhodes JM. 2000. Intracellular trafficking and release of intact edible mushroom lectin from HT29 human colon cancer cells. *Eur J Biochem*. 267:2122–2126.
Yu L-G, Fernig DG, Smith JA, Milton JD, Rhodes JM. 1993. Reversible inhibition of proliferation of epithelial cell lines by *Agaricus bisporus* (edible mushroom) lectin. *Cancer Res*. 53:4627–4632.
Yu L-G, Fernig DG, White MRH, Spiller DG, Appleton P, Evans RC, Grierson I, Smith JA, Davies H, Gerasimenko OV, et al. 1999. Edible mushroom (*Agaricus bisporus*) lectin, which reversibly inhibits epithelial cell proliferation, blocks nuclear localization sequence-dependent nuclear protein import. *J Biol Chem*. 274:4890–4899.
Zheng S, Li C, Ng TB, Wang HX. 2007. A lectin with mitogenic activity from the edible wild mushroom *Boletus edulis*. *Process Biochem*. 42:1620–1624.